DEPENDENCE OF TRANSPORT COEFFICIENTS ON PLASMA PARAMETERS IN THE TOKAMAK INSTALLATION

G. A. BOBROVSKIĬ, É. I. KUZNETSOV, and K. A. RAZUMOVA

Submitted April 16, 1970

Zh. Eksp. Teor. Fiz. 59, 1103–1114 (October, 1970)

The results are presented of a separate study of plasma transport coefficients on the TM-3 installation. The experimental diffusion and thermal conductivity coefficients are compared with theoretical formulas put forward by Galeev and Sagdeev. When the plasma density is high enough the experimental energy losses are found to be of the order of the classical values. In collisionless plasma there are considerable discrepancies with the classical theory and the electrical conductivity of the plasma is anomalously low. At relatively high electron temperatures ($T_e > 500$ eV) and low densities ($n_e < 6 \times 10^{12}$ cm^{-3}) we have observed protons whose temperature frequently cannot be explained by Coulomb energy transfer from electrons to ions. The anomalous resistance has been measured as a function of the plasma parameters in the hydrogen pressure range $p_0 \approx 10^{-4} - 10^{-3}$ Torr, using I = 7–35 kA and H_Z = 7–27 kOe.

INTRODUCTION

WE have used the Tokamak installation TM-3 to investigate transport processes in hydrogen plasma, including diffusion, thermal conductivity, electrical conductivity, and the rate of energy transfer from electrons to ions. The measurements were performed in a broad range of values of the parameters, namely, longitudinal magnetic field H_Z = 7–25 kOe, initial hydrogen pressure $p_0 = 10^{-4}$–10^{-3} Torr, and discharge current I = 7–35 kA. The discharge-current pulse in the TM-3 installation is trapezoidal in shape with fixed amplitude. The results reported here were obtained during the discharge period when the process could be regarded as stationary.

Separate measurements of the coefficients of diffusion and thermal conductivity on the TM-3 installation were reported in[1]. The diffusion losses were characterized by the lifetime τ_D of the charged particles in plasma. This was calculated from the derivative dn_e/dt of the electron density, corrected for the influx of electrons during the discharge process, which was due to the ionization of the hydrogen released by the walls. The total rate of energy loss (with the exception of losses by radiation or charge exchange) was characterized by the energy lifetime τ_e:

$$\tau_e = \frac{3}{2} nT \Big/ \left[jE - \frac{d}{dt}\left(\frac{3}{2} nT\right) - Q \right], \qquad (1)$$

where nT is the product of the density and the sum of electron and ion temperatures deduced from the diamagnetic effect, j is the current density, E is the electric field in the plasma, and Q is the total power lost by radiation and charge exchange and measured by semiconductor thermocouples and bolometers. The radius of the plasma column was assumed equal to the aperture in the partition restricting the discharge (a = 8 cm), and the radial distribution of all the quantities was assumed uniform.[1)]

[1)]The only exeption will be found in Sec. 3 of Ch. I.

Assuming the same distribution of density and temperature over the cross section of the plasma column, the quantity characterizing losses due to thermal conductivity τ_K was calculated from the relation

$$Z_{\text{eff}} = \sum_i n_i Z_i^2 \Big/ \sum_i n_i Z_i \qquad (2)$$

In all cases that are of interest in practice, τ_D is much greater than τ_ϵ and, therefore, the accuracy of τ_K is determined by the accuracy with which τ_ϵ is calculated.

It was found earlier[2] that the electrical conductivity σ_R of plasma measured in the hydrogen discharge of the TM-3 installation was, under most conditions, lower than the electrical conductivity σ calculated from the electron temperature T_e assuming a purely hydrogen plasma. The temperature T_e was determined from the measured diamagnetic effect and agreement with the diamagnetic measurements was obtained for results obtained from soft x-ray studies.[3] This has shown that the shape of the spectrum between 3 and 12 keV is not inconsistent with the Maxwellian electron energy distribution, whose temperature was in agreement with that obtained from diamagnetic measurements. The diamagnetic measurements of T_e, obtained with Tokamak T-3, have been confirmed by laser scattering experiments.[4]

The observed discrepancy between σ and σ_R can be associated with the presence of multiply ionized impurity atoms in the hydrogen plasma. Spectroscopic estimated of carbon and oxygen ion densities in the plasma with anomalous resistance have shown, however, that the effective charge of the plasma ions

$$1/\tau_e = 1/\tau_D + 1/\tau_\kappa.$$

(n_i and Z_i are the density and charge of the ions) does not exceed 2–3.[3] The measured values of the ratio η, on the other hand, are found to lie in the range 10–100. Such discrepancies cannot be explained even by purely carbon plasma with Z_{eff} = 4 (for the measured values of T_e and the electron density n_e the

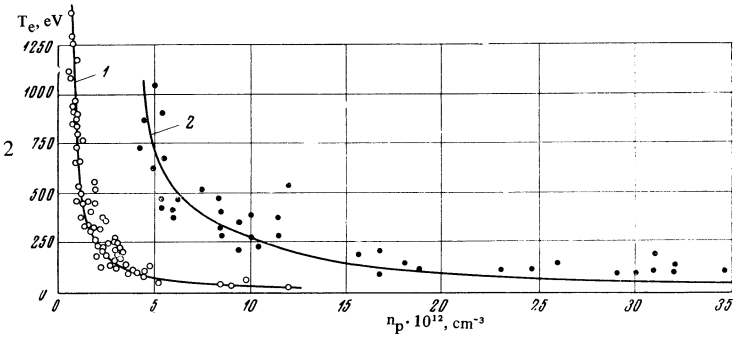

FIG. 1. Relation between T_e and n_e for fixed values of I: 1–I = 12 kA, H_z = 7–25 kOe; 2–I = 35 kA, H_z = 26 kOe.

ionization time of helium-like ions is considerably greater than the time taken by the process.

An independent method of estimating Z_{eff} is to measure the proton density by determining the attenuation of a hydrogen atomic beam by plasma at a beam particle energy of a few keV.[5] Under the conditions prevailing in the TM-3 installation this has led to a result which is not sufficiently accurate.

The absence of reliable measurements of the effective charge prevents us at present from estimating the contribution of impurities to the increase in the plasma resistance. We may conclude, nevertheless, that when the density n_e is low and the temperature T_e is high one does observe an anomalous plasma resistance which is due to the development of collective processes.

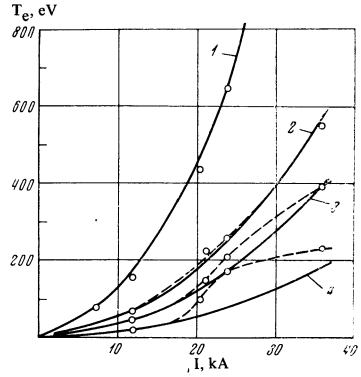

FIG. 2. Dependence of T_e on I for different n_e: 1–$n_e = 3 \times 10^{12}$ cm^{-3}; 2–$n_e = 6 \times 10^{12}$ cm^{-3}; 3–$n_e = 8 \times 10^{12}$ cm^{-3}; 4–$n_e = 13 \times 10^{12}$ cm^{-3}.

I. STUDIES OF PLASMA ENERGY LOSSES

1. Relation Between the Main Plasma Parameters and Some of its Consequences

Experiments performed on the Tokamak installations have shown that

$$T_e n_e^{\alpha} I^{\beta} = \text{const.} \tag{3}$$

Figure 1 shows the experimental values of T_e as a function of n_e obtained on TM-3 for two values of I. The solid curves represent the relation given by Eq. (3) for $\alpha \approx 1.4$ and $\beta = -2$. The two curves are normalized at the point $n_e = 5 \times 10^{12}$ cm^{-3}, T_e = 750 eV, I = 35 kA.

Therefore, Eq. (3) for TM-3 may be rewritten in the form

$$T_e n_e^{1.4} I^{-2} = \text{const.} \tag{3a}$$

This satisfies the experimental results in a broad range of values of the parameters. The only exception is provided by cases of high current and high density (see curve 2 in Fig. 1). The validity of this relation is naturally expected for the Tokamak installations if there is a relation between the heating and energy losses.

Equation (3) shows that we cannot arbitrarily vary any of the three parameters when the other two are fixed, i.e., functions of the form $f(n_e)$, $f(T_e)$, or $f(I)$ cannot be deduced from experiment. Thus, for example, if we set I = 12 kA (curve 1 in Fig. 1) then by neglecting radiation and using the empirical result for the electric field which is valid for the given current for small n_e

$$E = \text{const} \cdot T_e^{-1/2}, \tag{4}$$

we find from Eq. (1) that

$$\tau_\epsilon = \text{const} \cdot T_e^{3/2} n_e. \tag{5}$$

It follows from Eq. (3a), however, that Eq. (5) determines τ_ϵ to within the constant factor $(n_e^1 \cdot {}^4T_e)^m$, where m is an arbitrary number. When m = 0, Eq. (5) is identical with the empirical formula given in[2].

It follows from Eq. (3a) that when the density is constant $T_e \sim I^2$. The solid curves in Fig. 2 form a family of parabolas for different densities. The points joined by the broken curves represent the experimental data. At high densities (curve 4) T_e is found to increase with increasing current more rapidly than one would expect on the basis of Eq. (3a). From the plasma energy-balance equation given by Eq. (1), which may be written in the form

$$\tau_\epsilon \sim n_e T_e^{5/2} / j^2 \eta, \tag{6}$$

one would expect that this behavior of the temperature could be connected either with the relative increase in the energy input or with a change in the dependence of τ_ϵ on 0 at high densities. It is known from experiment (see Ch. II) that for large n_e we have $\eta \approx 1$ and does not vary with the current. It may therefore be concluded that $\tau_\epsilon(I)$ undergoes a change as we pass through higher densities so that $d \ln \tau_e / d \ln I$ increases.

The reduction in the rate of increase of the electron temperature (right-hand part of the broken curve 4 in Fig. 2) can therefore probably be explained by an increase in radiation losses. Bolometer measurements have shown that the radiated energy is negligible at low densities, whereas at high densities it increases up to 70% of the total input of energy into the plasma.

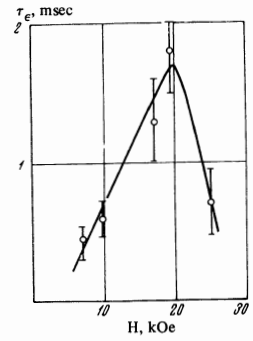

FIG. 3. Dependence of τ_ϵ on H_z; I = 7 kA. $n_e = 0.6 \times 10^{12}$ cm^{-3}, T_e = 500 eV.

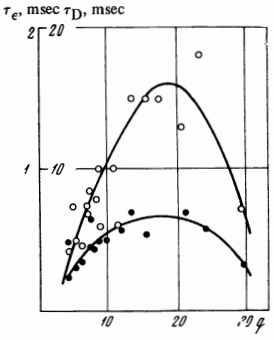

FIG. 4. Dependence of the lifetime on q at low densities: ○–τ_ϵ(q), ●–τ_D (q).

2. Transport Coefficients as Functions of Plasma Parameters

Let us now return to Fig. 1. It has been found that, to within experimental error, the $T_e(n_e)$ curves are practically independent of the longitudinal magnetic field H_z, i.e., as the latter is varied n_e and T_e shift along the curve. Hence, it follows that at constant current the n_e, T_e, H_z surface covered by the experimental points is a cylinder with generators perpendicular to the (T_e, n_e) plane. When it is cut by the $n_e = n_{e0}$ and $T_e = T_e(n_{e0})$ planes we obtain not a point but a line. This experimental result enables us, at least in principle, to deduce functions of the form $\tau(H_z)$ for fixed n_e, T_e, and I from the experimental data.

Figure 3 shows an example of the $\tau_e(H_z)$ curve for plasma with $\eta \gg 1$. Similar results are obtained for other discharge currents, except for the descending part which appears only for I < 10 kA. All this shows that practically throughout the range of parameters which we are considering the quantity τ_ϵ increases with increasing H_z. If we know the functions $\tau_\epsilon(H_z)$ for different I we can obtain a formal construction for τ_ϵ as a function of the stability factor q. The function $\tau_\epsilon(q)$ is plotted in Fig. 4. However, the experimental data included in this graph correspond to the same temperature but different densities. Subject to this, it may be said that the energy lifetime increases with increasing q up to a certain limit ($q \approx 20$) and then decreases. This effect is probably not difficult to explain if we recall that for large q and finite plasma conductivity it becomes more difficult to equalize the electric potentials along the magnetic lines of force.

Since Eq. (3a) does not involve the magnetic field, it follows that [see Eq. (6)] $\tau_\epsilon(H_z)$ w $1/\eta(H_z)$, i.e., when $\eta \gg 1$ the losses increase with increasing degree of anomaly.

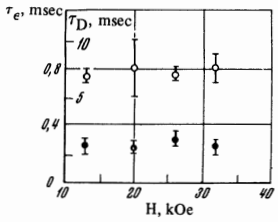

FIG. 5. Lifetimes for different H_z with I = 24 kA, $n_e = 1 \times 10^{13}$ cm^{-3}, T_e = 250 eV: ○–$\tau_\epsilon(H_z)$, ●–$\tau_D(H_z)$.

When $\eta \approx 1$ the energy lifetime is independent of the longitudinal magnetic field (Fig. 5). The independently measured diffusion lifetime often behaves by analogy with τ_ϵ:

1) the dependence of τ_D on q (Fig. 4) is similar to the function $\tau_\epsilon(q)$;

2) when $\eta \approx 1$ the diffusion lifetime is independent of the magnetic field (Fig. 5).

However, the dependence of τ_ϵ and τ_D on n_e, for example, is different.

We may thus conclude from the above three independent experimental relations, namely, $T_e = T_e(n_e, I)$, $\tau_\epsilon = \tau_\epsilon(H_z, I)$,[2)] and $\tau_D = \tau_D(H_z, I)$ that the laws governing the transport coefficients in plasma are different at low and high densities for which $\eta \gg 1$ and $\eta \approx 1$, respectively.

3. Comparison of Experimental and Theoretical Transport Coefficients

The transition from the local theoretical transport coefficient[6] to the integrated plasma characteristics can be achieved by using the formulas

$$\tau_D = a^2 / (2.4)^2 D, \tag{7}$$

$$\tau_\varkappa = a^2 / (2.4)^2 \varkappa, \tag{8}$$

where a is the radius of the plasma column and D and κ are the diffusion and thermal conductivity coefficients. These formulas are based on the assumption that the distribution of all the plasma parameters over the cross section of the column takes the form of a Bessel function of order zero if the transport coefficients do not vary in the radial direction. The values of n_e, T_e, and H_z, averaged over the cross section of the plasma column, were used in calculating D and κ. The magnetic field due to the current was calculated for the boundary of the plasma column assuming that the radius of the column was a = 8 cm. The difference between the assumed distributions and the real distributions may increase the discrepancy between experiment and theory to within a factor of three.

It follows from the theoretical analysis[6] that plasmas in toroidal installations can be divided into three collision frequency regions, as follows:

1) The region of collisionless plasma $\nu/\nu_1 < 1$, where $1/\nu_1$ is the period of drift motion of trapped particles. In this region the transport coefficients increase by a factor of $\epsilon^{-3/2}$ because of the presence of the trapped particles (ϵ is the ratio of the minor to the major radii of the torus) as compared with the values obtained by Pfirsch and Schlüter.[7]

2) The transition region $1 < \nu/\nu_1 < \epsilon^{-3/2}$. This is

[2)] In calculating τ_ϵ we used, in addition to n_e, T_e, and I, one more independent parameter, namely, the electric field E [see Eq. (1)].

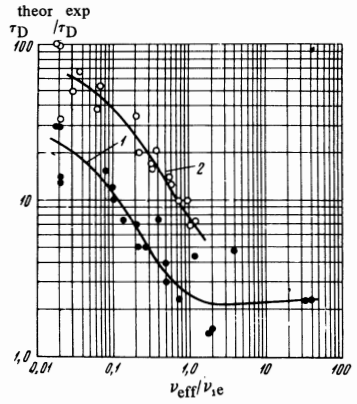

FIG. 6

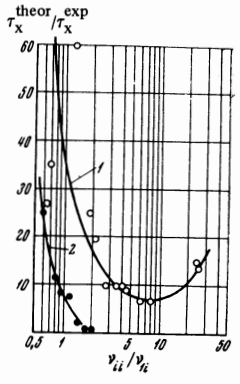

FIG. 7

FIG. 6. Ratio of calculated to measured lifetime τ_D as a function of ν_{eff}/ν_{ie}: curve 1–I = 10 kA, H_z = 12 kOe; curve 2–I = 24 kA, H_z = 13-32 kOe.

FIG. 7. Ratio of calculated to measured lifetime τ_K as a function of ν_{ii}/ν_{ii}: curve 1–I = 10 kA, H_z = 13 kOe, curve 2–I = 35 kA, H_z = 27 kOe.

characterized by the absence of the dependence of the transport coefficients on the collision frequency.

3) The region of collisional plasma $\nu/\nu_i \gg \epsilon^{-3/2}$. Here the hydrodynamic Pfirsch-Schlüter approximation is valid. In view of this distribution, it is meaningful to consider the lifetime τ as a function of the collision frequency and not as a function of n_e and T_e.

Figure 6 shows the ratio of the theoretical lifetime calculated from Eq. (7) to the experimental τ_D under two conditions. The dimensionless frequency ν_{eff}/ν_{ie} calculated from electrical conductivity measurements is plotted along the horizontal axis.

When $\eta \approx 1$ the frequency ν_{eff} is not very different from the electron-ion collision frequency. It is clear from the figure that, as the collision frequency increases, the difference between theory and experiment, which occurs in the collisionless region, is found to decrease.

Figure 7 shows the ratio of the theoretical lifetime calculated from Eq. (8) to the experimental lifetime τ_K^{exp} (see Fig. 2) as a function of the dimensionless ion-ion collision frequency ν_{ii}/ν_{ii}. The theoretical ion thermal conductivity coefficient is very dependent on T_i. It is shown in Section 2 of Chap. II that non-Coulomb heating of a small fraction of the ions occurs in the collisionless plasma region. Under these conditions the ion thermal conductivity was calculated for the cold ion mass. As we pass into the collisionless plasma region, the measured energy losses increase rapidly in comparison with the theoretical values.

II. ANOMALOUS RESISTANCE

The region of electron densities and temperatures in which the anomalous resistance is observed can be seen in Fig. 1. The quantity η increases with decreasing density and, consequently, with increasing electron temperature, i.e., on the left-hand part of the $T_e(n_c)$ curve. When the discharge current is large the anomalous region shifts toward higher densities.

1. Characteristics of the Anomalous Resistance

It was noted in[8] that η was a rapidly varying function of the ratio ω_{He}/ω_{pe} (ω_{He} and ω_{pe} are the Larmor and plasma electron frequencies) which is proportional to $H_z n^{-1/2}$. These experimental data cannot, however, be used to conclude that the anomalous plasma resistance at a fixed density is a rapidly varying function of H_z. In fact, and this was noted above (Sec. 2 of Ch. I), both n_e and T_e vary with varying H_z [remaining on the same $T_e(n_e)$ curve] under the conditions of anomalous resistance. It is shown in Sec. 2 of Ch. I that, for given n_e and T_e, we have $\eta(H_z) \propto 1/\tau_e(H_z)$, and the quantity η is a slowly varying function of H_z when this quantity lies between 7 and 27 kOe.

According to modern ideas, the appearance of anomalous resitance in plasma is possible in the presence of ion-acoustic instability.[9] This instability appears in nonisothermal hydrogen plasma for $u/v_{th} > 2 \times 10^{-2}$, where u and v_{th} are the drift and thermal velocities of the electrons. There is, therefore, interest in the dependence of the ratio u/v_{th} on the plasma parameters.

It follows from Eq. (3) that

$$u / v_{th} = \text{const} \cdot T_e^{1/2} I^{-1/2}. \quad (9)$$

The experimental values of u/v_{th} turn out to be much greater than 0.02 (or $u/c_s \gg 1$, where c_s is the velocity of sound) and are independent of the magnetic field H_z within the range of error. The spread of the experimental points is such that u/v_{th} may be proportional to $H_z^{1/m}$, where m lies between 3 and 4.

It follows from Eq. (9) that for high temperatures T_e the ratio u/v_{th} is almost independent of temperature. For a given current, this means that

$$\eta \propto E / E_{cr}, \quad (10)$$

where E is the longitudinal electric field in the plasma and E_{cr} is the Dreicer field. The region given by (10) was reported earlier in[2]. It is valid for $\eta \gg 1$ in electric fields in excess of the critical value and cannot be modified by impurities because the effective charge enters both ratios in the same way.

The phenomenon of anomalous resistance has also been observed in Stellarator C. During the conference on closed systems (Dubna, 1969) Dr. E. Mazzucato reported a comparison between anomalous resistance studies carried out on Stellarator C and Tokamak TM-3. Figure 8 repeats this graph but has been augmented by new data obtained on TM-3 and T-3. The ratio $\sigma/\sigma_R \equiv \eta$ is plotted along the ordinate axis and the ratio u/v_{th} along the abscissa axis. The experimental points referring to Stellarator C are taken from[10]. The points referring to TM-3 were obtained for current densities j = 35–180 A/cm^2 and different magnetic fields and densities.

The points referring to T-3 are taken from[11]. It follows from Fig. 8 that the experimental points obtained for different installations occupy a common region. Moreover, we note that there are a number of states in the TM-3 installation (these were obtained with minimum current density and particle density in the range $10^{12} - 2 \times 10^{12}$ cm^{-3}) for which, despite the

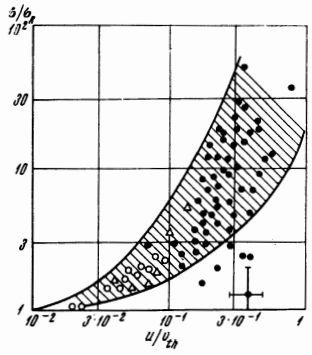

FIG. 8

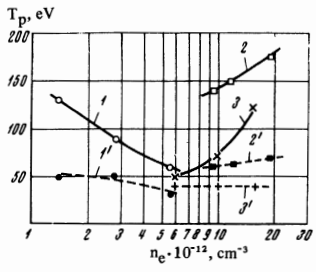

FIG. 9

FIG. 8. Ratio $\sigma/\sigma_R \equiv \eta$ as a function of u/v_{th}: ○–Stellarator C, △–Tokamak T-3, ●–TM-3.

FIG. 9. Ratio of the temperatures of the hot (solid curves) and cold (broken curves) proton components as functions of electron density: curves 1 and 1′–I = 11 kA, H_z = 10 kOe (anomalous resistance); 2 and 2′–I = 35 kA, H_z = 27 kOe; 3 and 3′–I = 20 kA, H_z = 20 kOe (curve 3 was given in [2]).

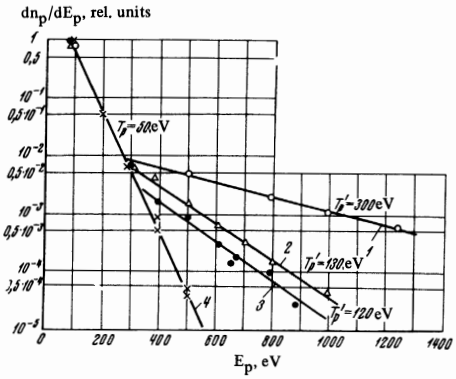

FIG. 10

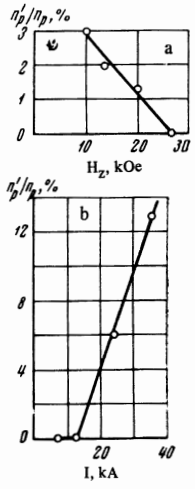

FIG. 11

FIG. 10. Proton energy spectra for different longitudinal magnetic fields, I = 12 kA, hydrogen pressure $p_0 = 3 \times 10^{-1}$ mm Hg; curve 1–H_z = 10 kOe, 2–H_z = 14 kOe, 3–H_z = 18 kOe, 4–H_z = 26 kOe.

FIG. 11a. Fraction of hot protons as a function of H_z for I = 12 kOe, $p_0 = 3 \times 10^{-4}$ mm Hg H_2; b–fraction of hot protons as a function of I for H_z = 26 kOe, $p_0 = 4 \times 10^{-4}$ mm Hg H_2.

large value of the ratio u/v_{th}, the anomalous resistance is very weakly defined (points outside the marked region in Fig. 8).

2. Heating of Protons in the Presence of Anomalous Resistance

Measurements of the ion energy distribution in the Tokamak installations have been carried out by the well-known method of energy analysis of neutral hydrogen atoms in the range between 100 eV and a few keV.[12] Energy spectra obtained in this way are usually interpreted as the superposition of Maxwellian distributions with different temperatures (see, for example,[2]). The higher temperature T_p' is usually ascribed to protons localized at the center of the plasma column and the lower temperature T_p to protons in the peripheral region. For states corresponding to the right-hand branch of the $T_e(n_e)$ curve the quantity T_p' is not inconsistent with the hypothesis that the heating of protons is due to Coulomb energy transfer from electrons. Under these conditions, the temperature of the hot protons increases with increasing electron density (Fig. 8, curves 2 and 3).

In states showing anomalous resistance, which correspond to the left-hand branch of the $T_e(n_e)$ curve, the proton energy spectra practically always retain the same form, but the dependence on the electron density is now opposite to that indicated above. Figure 9 (curve 1) shows an example of this relation. As the electron density increases the hot-proton energy is found to decrease.

Figure 10 shows the proton spectra for different magnetic fields in the presence of anomalous resistance. When the field is high enough hot protons are not formed. A similar phenomenon involving the disappearance of the hot protons occurs when the discharge current is reduced.

Figure 11 shows the fraction of hot protons as a function of the magnetic field and the discharge current. It was assumed that the spectrum was also formed by the superposition of two Maxwellian distributions. It is important to note that when the hot protons disappear the anomalous resistance persists and the magnitude of η under these conditions is about 10.

The value of the temperature T_p' in the presence of the anomalous resistance, and the dependence on the parameters described above, are in clear conflict with the Coulomb mechanism of proton heating. Simple calculations show that the influx of heat from electrons, even in the absence of energy losses by protons, is insufficient for heating the latter to the temperature T_p'. When losses due to charge transfers and classical thermal conductivity of protons are taken into account the Coulomb mechanism turns out to be sufficient only for heating the protons up to the temperature T_p. It can also be shown that, at least in certain states with anomalous resistance, the proton energy spectrum does not reflect the corresponding spatial temperature distribution. Thus, for a state corresponding to curve 1 in Fig. 10 the fraction of hot protons amounts to about 3%. The maximum radius of the region with hot protons assuming homogeneous neutral hydrogen atom distribution over the cross section of the column, should be about 2 mm, i.e. of the order of the proton Larmor radius, which is obviously impossible.

We must, therefore, conclude that in states with anomalous resistance there is a non-Coulomb mechanism for the heating of a small fraction of the plasma protons.

3. Discussion

It is shown at the end of Ch. I that transition to states with anomalous resistance is accompanied by a loss of energy in comparison with the value determined by the classical transport coefficients in toroidal systems.

If we try to combine all the above results into a single picture we must conclude that in states with low

densities and high electron temperatures there is an instability which leads to an increase in the effective electron collision frequency and to the heating of a fraction of the protons to substantial temperatures as well as to an increase in the thermal conductivity and diffusion.

In states with anomalous resistance there are conditions which favor the development of ion-acoustic instability. As far as we know, there is no theory of anomalous resistance which assumes the development of this instability for $\omega_{He} > \omega_{pe}$ and satisfactorily explains all the experimental data.

On the other hand, we must note the following experimental facts which were established on the Tokamak installation:

a) in the region of anomalous resistance the energy lifetime increases with increasing H_z and decreasing I (Fig. 4);

b) high-energy protons disappear under these conditions for sufficiently high H_z and sufficiently low I (see Fig. 11);

c) high-energy protons were found earlier in[12] at a time corresponding to the development of hydromagnetic instability[13] in discharges with $q \lesssim 3$, where q is the stability factor.

These facts lead us to the hypothesis that both increased plasma losses and hot protons may appear for $q > 3$ in low-density plasma due to a weakly defined (in comparison with $q \lesssim 3$) magnetohydrodynamic instability. For example, one might assume that, as the plasma column becomes modified, conditions are set up which are favorable for the development of ion-acoustic or some other instability leading to the above effect.

CONCLUSION

We have shown that the behavior of plasma is different in regions with low and high density. In the former region, where anomalous resistance is clearly defined, we find the following:

1) The temperature is a rapidly varying function of density.

2) The relation given by (3a) is well satisfied.

3) The measured transport coefficients are much greater than those calculated from classical theory.

4) The transport coefficients depend on q.

5) The ion thermal conductivity cannot account for the observed losses (the transfer of energy from electrons to ions is sufficient under all conditions to ensure losses with classical ion thermal conductivity). If we do not assume an enhanced (in comparison with the Coulomb) heat transfer from electrons to ions we may conclude that the losses are determined by the electron thermal conductivity. The same conclusion is reached if some type of instability develops under these conditions without more intensive heating of the ions.

6) The ratio u/v_{th} is related to the current and the electron temperature by the empirical relation given by Eq. (9) and is found to be almost constant at sufficiently high temperatures.

7) In most states with anomalous resistance $u/v_{th} \gg 2 \times 10^{-2}$ or $u/c_s \gg 1$.

8) When the experimental data are plotted in the form of σ/σ_R as a function of u/v_{th}, the results obtained for the Tokamak and Stellarator C installations are found to lie in a common region.

9) For densities of $10^{12} - 2 \times 10^{12}$ cm^{-3} and current densities $j \approx 35$ A/cm^2 there are states in which, in spite of the high value of u/v_{th}, the anomalous resistance is very weakly defined.

10) There is a fraction of hot protons whose temperature is in conflict with the Coulomb mechanism of heating by electrons.

In high-density plasma without high anomalous resistance it is found that

1) the temperature is a slowly varying function of density;

2) T_e is greater than predicted by (3a);

3) the dependence of τ_e on I is different from that in the first region;

4) the transport coefficients are in better agreement than the theoretical values (as noted above, it is difficult to speak of an agreement for the functional dependence on the plasma parameters);

5) the transport coefficients are independent of the magnetic field;

6) most of the losses can be explained by the ion thermal conductivity.

We must also note that, in the case of high-density plasma, the heating of most of the ions is not inconsistent with the hypothesis that the ions receive energy as a result of Coulomb collisions with electrons.

We are indebted to L. A. Artsimovich, V. S. Mukhovatov, L. I. Rudakov, and V. S. Strelkov for useful discussions, to Yu. S. Maksimov for placing the semiconductor bolometers at our disposal, and to L. S. Efremov and A. A. Kondrat'ev for assistance in the experiments.

[1] G. A. Bobrovskiĭ, N. D. Vinogradova, É. I. Kuznetsov, and K. A. Razumova, ZhETF Pis. Red. 9, 269 (1969). [JETP Lett. 9, 158 (1969)].

[2] L. A. Artsimovich, G. A. Bobrovskiĭ, E. P. Gorbunov, et al., Plasma Phys. and Contr. Nucl. Fusion Res. Vol. 1, IAEA, Vienna, 1969, p. 157.

[3] D. A. Shcheglov, ZhETF Pis. Red. 6, 949 (1967) [JETP Lett. 6, 365 (1967)].

[4] N. J. Peacock, D. C. Robinson, M. J. Forrest, P. D. Wilcock, and V. V. Sannikov, Nature 224, 488 (1969).

[5] V. V. Afrosimov, B. A. Ivanov, A. I. Kislyakov, and M. P. Petrov. Zh. Tekh. Fiz. 36, 89 (1966). [Sov. Phys.-Tech. Phys. 11, 63 (1966)].

[6] A. A. Galeev and R. Z. Sagdeev, Zh. Eksp. Teor. Fiz. 53, 348 (1967) [Sov. Phys.-JETP 26, 233 (1968)].

[7] D. Pfirsch and A. Schlüter, Rep. Max Plack Inst., Munich, MPI/PA/7/67, 1967.

[8] G. A. Bobrovskiĭ, K. A. Razumova, and J. A. Sceglov, Plasma Physics 10, 436 (1968).

[9] B. K. Zavoĭskiĭ and L. I. Rudakov, Atomnaya Energiya 23, 417 (1967).

[10] I. G. Brown, D. L. Dimock, E. Mazzucato, M. A. Rothman, R. M. Sinclair, and K. M. Young, Plasma Phys. and Contr. Nucl. Fusion Res. 1, IAEA, Vienna, 1969, p. 497.
[11] E. P. Gorbunov, S. V. Mirnov, and V. S. Strelkov, Nucl. Fusion 10, 43 (1970).
[12] V. V. Afrosimov and M. P. Petrov, Zh. Tekh. Fiz. 37, 1995 (1967). [Sov. Phys.-Tech. Phys. 12, 1467 (1968)].
[13] E. P. Gorbunov and K. A. Razumova, Atomn. énerg. 15, 363 (1963).

Translated by S. Chomet
127